Effective Detection of Brain Cancers using Optimized Deep Learned CAD Models

[1]Deepak V.K,

[1]Research Scholar, Department of Electronics & Communication, Noorul Islam Centre for Higher Education, Thuckalay, Kumaracoil, Tamilnadu.

deepakvk2@gmail.com

[2]Dr.Sarath. R

[2]Associate Professor, Department of Electronics &Instrumentation, Noorul Islam Centre for Higher Education, Thuckalay, Kumaracoil, Tamilnadu.

sarathraveendran@gmail.com

ABSTRACT

Brain cancer continues to be among the leading causes of death for both men and women and much effort have been expended in the form of screening programs for prevention. Given the exponential growth in the number of MRI collected by these programs, computer-assisted diagnosis has become a necessity. Computer-assisted detection techniques developed to date to improve diagnosis without multiple systematic readings have not resulted in a significant improvement in performance measures. In this context, the use of automatic image processing techniques resulting from deep learning represents a promising avenue for assisting in the diagnosis of brain cancer. In this paper, present a deep learning approach based on a Convolutional Neural Network (CNN) model for brain tumor classification. The proposed approach aims to classify the brain tumors in to different grades. Experimental results on MRI images using the BRATS dataset show that the HHO-CNN model achieved high processing performances with 97% of accuracy in the proposed classification task when compared with other classification techniques and state-of-the-art models.

***Keywords**: CNN, HHO, SVM, BOVW.*

1. INTRODUCTION

The advancement in medical technologies helps the clinical experts to facilitate more efficient e-health care systems to the patients. There is a number of medical domains where e-health care systems are beneficial [1]. Computer vision-based applications of biomedical imaging are gaining more importance as they provide recognition information to the radiologist for batter treatment-related problems. Different medical imaging techniques and methods that include X-ray, Magnetic Resonance Imaging (MRIs), Ultrasound, and Computed Tomography (CT), have a great influence on the diagnosis and treatment process of patients. The formation of abnormal groups of cells inside the brain or near it leads to the initialization of a brain tumor. These abnormal cells affect the health of the patient and abrupt the processing of the brain [2]. The most common type of brain tumor known as Astrocytoma arises from the astrocyte cells, which form part of the brain's supportive (neuroglial) tissue. An astrocytoma develops from star-shaped glial cells (astrocytes) that support nerve cells. These tumors can be located anywhere in the brain, but the most common location is in the frontal lobe. Astrocytomas are the most common primary CNS tumor. The physician, usually the neurosurgeon or neuro-oncologist, will discuss the type and location of an astrocytoma. The pathologist will assign it a grade. Astrocytomas are generally classified as low or high grade. Low-grade astrocytomas are slow growing. High-grade astrocytomas (grades three and four) grow more quickly. The characteristics of an astrocytoma vary depending on the tumor’s grade and location. Most people are functioning normally when diagnosed with a low-grade astrocytoma [3-5]. Symptoms tend to be subtle and may take one to two years to diagnose. This is because the brain can often adapt to a slow-growing tumor for a period of time. High-grade tumors may present with changes that are sudden and dramatic. Brain imaging analysis, diagnosis, and treatment with adopted medical imaging techniques are the main focus of research for the researcher, radiologist and clinical experts. A variety of image-processing techniques and methods have been used for the diagnosis and treatment of a brain tumor. The development of new technologies, especially artificial intelligence and machine learning, has had a significant impact on medical field, providing an important support tool for many medical branches, including imaging. Different machine-learning methods for image segmentation and classification are applied in MRI image processing to provide radiologists with a second opinion. In the field of computational medical imaging, methods of deep convolutional neural networks (CNN) [6] have proved successful for the hierarchical unsupervised learning of imaging features of increasingly complex data directly from raw images, allowing discovering the relevant characteristics, instead of extracting features defined a priori by the user. The remainder of this paper is divided into four sections. After introducing, related works on brain cancer classification are reviewed in Section 2. Section 3 presents the proposed HHO based CNN model for brain tumor classification. Experiments, results and comparison with popular CNNs models are detailed in Section 4. Finally, this paper is concluded in Section 5.

2. RELATED WORKS

Research related to the detection of brain cancer has increased during the last decade. Much work has been directed towards the detection of the presence of cancerous tissue in the brain and the classification of tumors. Some researchers have preferred to design aided diagnosis

systems based on Content based image retrieval techniques that would have the advantage of offering radiologists images available in a medical image database, whose content is known and which would be similar to image request for which the radiologist would have doubts. However, this approach also raises problems of search time and adequate similarity measurement between the request image and those contained in the database.

S. Chaplot et al. [7] proposed a novel strategy for the classification of magnetic resource images of human brain which utilizes wavelets as contribution to support vector machine and neural system self-organizing maps. The proposed technique orders MR brain images as abnormal or normal. Their proposed approach has a dataset of 52 MR brain images. A rate of over 94% was achieved with the self-organizing maps (SOM) whereas and 98% using the support vector machine method. It was observed that the classification rate is high for a support vector machine classifier if compared with a self-organizing map-based approach.

M. Maitra et al. [8] proposed new approach for mechanized diagnosis, for the classification of MRI images. The proposed strategy is seemingly a variant of orthogonal discrete wavelet transform (DWT), called Slantlet transform for highlight extraction. Here, a 2-D MR picture processes its intensity histogram and then connected to Slantlet transform as its histogram flag. At that point an element vector is made by considering the sizes of Slantlet transform yields comparing to six positions which are supposed to be spacial, picked by a particular rationale. The components which are extricated used to prepare a neural system based classifier. The fundamental reason for classifier is to arrange the pictures either as typical or unusual for Alzheimer's sickness. From this strategy, they accomplished the productivity of 100% in accurately characterizing the Alzheimer's malady.

Y. Zhang et al. [9] proposed a hybrid technique in light of forward neural network (FNN) to group MR brain images. The proposed strategy initially utilized the discrete wavelet transform in order to extract main features from MR Images and after that applied the principal component analysis technique to diminish feature space to a limit. The diminished components were sent to a forward neural network (FNN), where the parameters were upgraded utilizing an improved artificial bee colony algorithm (ABC) calculation in view of both fitness scaling and chaotic theory.. At that point, K-fold cross validation technique was utilized to maintain a strategic distance from over fitting. The outcomes demonstrate that SCABC can acquire the minimum mean MSE and 100% accuracy.

JankiNaik et al. [10] introduced a proposed method to classify the medical images for diagnosis. Here, preprocessing, feature extraction, association rule mining and classification are the steps involved. Someexperiments with MRI images for tumor detection is carried out here. Preprocessing has been done with the help of median filtering process. After that, essential features have been extracted with texture feature technique. Then mining of association rules is done from extracted feature using Decision Tree classification algorithm. They concluded that the proposed method improves the efficiency of classification of CT scan images than traditional methods.

Y. Zhang et al. [11] proposed a novel method for classify brain MRI images as either normal or abnormal by using SVM and DWT (Discrete Wavelet Transform) approach. PCA (Principal Component Analysis) approach also used to diminish the no. of features extracted by Wavelet Transform. These methods were applied on 160 MR Brain Images for detection

of Alzheimer's disease with four different kernels and achieved maximum accuracy for GRB kernel of 9.38%.

brain tumor segmentation and categorization were mentioned by Mathew et al. [12] using the discrete wavelet transform, GLCM and Gabor wavelet. In the beginning, the thresholding of Ostu is utilized in the pre-processing section. K-means clustering is used to discover the tumor part from brain MR images. Likewise, the features were gotten from the GLCM, DWT and Gabor wavelet. For the feature set reduction, the PCA is used. Finally, the tumor part is categorized as malignant or benign with the help of a support vector classifier (SVM). In this portion, the RBF kernel, linear kernel, and polynomial kernel were used. The observational outcomes had displayed that the linear kernel is given better performance when compared to others.

The segmentation of the brain tumor was deliberated by Iqbal et al. [13] in the multi-spectral MR pictures with the support of convolutional neural networks. The current inspection provides a practical system manner for the brain tumor separation through the multi-modular pictures. With the growing level of accomplishment, this article presented three dissimilar models. The results prove that the intermediate convolutional maps and use of interpolation procedures were successful technology and also yield the possible outcomes. Different deep networks are discussed that required training to congregate. By the by, the suggested system framework is little, quick and required less memory.

Sharif et al. [14] presented an active deep learning system for the segmentation and classification of brain tumors. They initially performed contrast enhancement, and the resultant image was passed to the Saliency-based Deep Learning (SbDL) method, for the construction of a saliency map. The thresholding was applied in the next step, and the resultant images were used to fine-tune the pre-trained CNN model Inception V3. Further, they also extracted dominant rotated local binary pattern (DRLBP) features, fused with CNN features. Later on, a PSO-based optimization was performed and the optimal vector was passed to the Softmax classifier for final classification. They used BRATS 2015, 2017, and 2018 datasets for evaluation, and achieved improved classification accuracy. Other methods were also introduced in the literature for brain tumor classification, such as a generative adversarial network artificial neural network (ANN)-based learning [15], ELM-based learning [16], residual network [17], standard-features-based classification [18,19], adaptive independent subspace analysis [20], transfer learning-based tumors classification [21], and Excitation DNN [22]. Deep learning refers to advanced statistical learning methods organized in multiple layers, to extract representations of data on multiple levels, and whose layers are not predefined by the user but learned directly from the data by the algorithm, thus mimicking human neuronal functioning [10]. It has been successfully applied to various pathologies and modalities, including the use of convolutional networks (CNN) that exploit large databases for the extraction of relevant descriptors and segmentation [11]. The main challenge of cancer automatic aided diagnosis systems is dealing with the inherent complexity of MRI images. To deal with this, choose to use a powerful HHO based convolutional neural network of multiclass classification problem. Here use the ResNet model [12], one of state of the art in the image recognition competition ImageNet [13]. The ResNet is built for natural images processing but modified it to deal with MRI images for brain cancer classification using transfer learning.

3. PROPOSED CNN MODEL FOR MULTI-CLASS BRAIN CANCER CLASSIFICATION

The CNN model structure is simpler and easier to expand than the neurocognitive machine. In the neurocognitive machine, the downsampling layer and the convolutional layer alternate to form the function of feature extraction and abstraction, while in the convolutional neural network, the convolutional layer and the downsampling layer alternate, and their functions are similar. The convolution operation simplifies feature extraction, the excitation function replaces multiple nonlinear functions of the neurocognitive machine, and the pooling operation is also simpler [23]. The CNN architecture is shown in Figure 1.

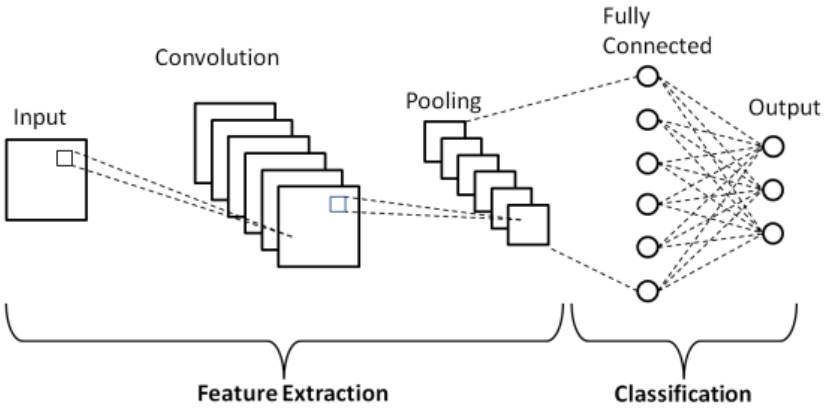

Figure 1: CNN architecture

CNNs are mostly used for deep neural networks. This consists of several nonlinear levels of operation, such as neural networks with many hidden layers. It can view images and frames from the film. CNNs learn the connections between pixels in the input image by extracting reflective attributes through pooling and convolution methods. The characteristics of each layer utilizing trained kernels differ in complexity, with simple elements like the edges extracted in the first layer and high level features extracted in the later layers. [24].

A CNN is composed of several kinds of layers:

- Convolutional layer: creates a feature map to predict the class probabilities for each feature by applying a filter that scans the whole image, few pixels at a time.
- Pooling layer (downsampling): scales down the amount of information the convolutional layer generated for each feature and maintains the most essential information (the process of the convolutional and pooling layers usually repeats several times).
- Fully connected input layer: “flattens” the outputs generated by previous layers to turn them into a single vector that can be used as an input for the next layer.
- Fully connected layer: applies weights over the input generated by the feature analysis to predict an accurate label.
- Fully connected output layer: generates the final probabilities to determine a class for the image.

The convolutional layer is composed of a set of convolutional kernels where each neuron acts as a kernel. However, if the kernel is symmetric, the convolution operation becomes a correlation operation. Convolutional kernel works by dividing the image into small slices, commonly known as receptive fields [25]. Convolution operation can be expressed as follows:

$$f_1^k(p,q) = \sum_c \sum_{x,y} i_c(x,y) \,.\, e_1^k(u,v) \qquad (1)$$

Where, $i_c(x,y)$is an element of the input image tensor I_c , which is element wise multiplied by $e_1^k(u,v)$ index of the k[th] convolutional kernel k_1 of the l[th] layer. Whereas output feature-map of the k[th] convolutional operation can be expressed as $F_1^k = [f_1^k(1,1), \dots (f_1^k(p,q), .. f_1^k(P,Q))]$.

In pooling layer once features are extracted, its exact location becomes less important as long as its approximate position relative to others is preserved. Pooling or down-sampling is an interesting local operation. It sums up similar information in the neighborhood of the receptive field and outputs the dominant response within this local region

$$Z_l^k = g_p(F_l^k) \qquad (2)$$

Equation (2) shows the pooling operation in which Z_l^k represents the pooled feature-map of l[th] layer for k[th] input feature-map F_l^k , whereas g_p (.) defines the type of pooling operation.The use of pooling operation helps to extract a combination of features, which are invariant to translational shifts and small distortions. The activation function for a convolved feature-map is defined in equation (3).

$$T_l^k = g_a(F_l^k) \qquad (3)$$

The above equation $F_l^k$is an output of a convolution, which is assigned to activation function g_a (.) that adds non-linearity and returns a transformed output $T_l^k$for lth layer.

Batch normalization is used to address the issues related to the internal covariance shift within feature-maps. The internal covariance shift is a change in the distribution of hidden units' values, which slows down the convergence (by forcing learning rate to small value) and requires careful initialization of parameters. Batch normalization for a transformed feature-map $F_l^k$is shown in equation (4).

$$N_l^k = \frac{F_l^k - \mu_B}{\sqrt{\sigma_B^2 + \varepsilon}} \qquad (4)$$

In equation (4), N_l^k represents normalized depict mean andμ_B and σ_B^2feature-map, F_l^k is the input feature-map, B variance of a feature-map for a mini batch respectively. Dropout introduces regularization within the network, which ultimately improves generalization by randomly skipping some units or connections with a certain probability. Various Activation Functions have been used in the, they are

1) Rectified linear units (ReLU)

It is used in deep neural nets. Recently it has been shown to have six times improved convergence from the function of Tanh. Mathematically, Rectified liner units represented as:

$$R(x) = max\,(0,x)$$

$$\text{If } x < 0, R(x) = 0 \; and \; x >= 0, R(x) = x$$

2) Hyperbolic Tangent function- Tanh

Here, the output is zero based, since the range between -1 and 1. Optimization in this approach is easier therefore it is often favoured in practice over sigmoid function. Mathematically, Tanh represented as:

$$f(X) = \frac{1 - \exp(-2x)}{1 + \exp(-2x)} \qquad (5)$$

3) Sigmoid Activation function

The range of sigmoid function is in between zero and 1. It is represented by S-shaped curve. Mathematically, it is represented as:

$$f(X) = \frac{1}{1 - \exp(-x)} \qquad (6)$$

ResNet50

ResNet50 is a 50-layer Residual Network with 26M parameters. The residual network is a deep

convolutional neural network model that is introduced by Microsoft in 2015 [26]. In Residual network rather than learning features, we learn from residuals that are subtraction of features learned from the layer's inputs.

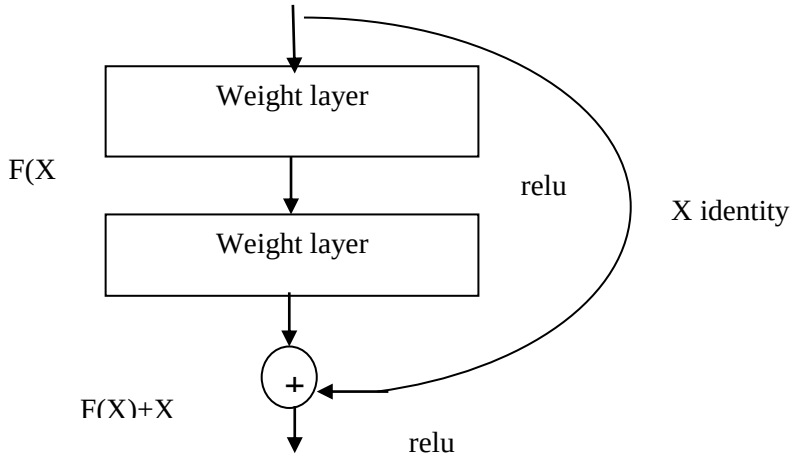

Figure 2: Residual learning building blocks

ResNet used the skip connection to propagate information across layers. ResNet connects nth layer input directly to some (n+x)th layer which enables additional layers to be stacked and a to establish a deep network. We used a pre-trained ResNet50 model in our experiment and fine-tuned it. In Figure 2, the architecture of ResNet50 is shown.

The model has flattened layer, which is followed by densely connected neurons. Some of the perceptron has been dropped off in order to prevent overfitting. The loss function utilized the "binary_crossentropy" whereas the optimiser is HHO. In deep neural networks, apply different optimization methods by adjusting parameters such as weights and learning rates to reduce the loss. Here used the Harish Hawks Optimizer (HHO), proposed by Heidari et al. in 2019 [20]. Harris Hawks Optimization (HHO) is a novel nature-inspired, gradient-free, and population-based optimization algorithm that imitates the chasing style of Harris Hawks' birds. The proposed block diagram of HHO based CNN is shown in figure 3

- **Harris Hawks Optimization**

  Harris Hawks Optimization (HHO) is a novel nature-inspired, gradient-free, and population-based optimization algorithm that imitates the chasing style of Harris Hawks' birds. HHO was

introduced recently by Heidari et al. in 2019 [27]. The algorithm follows the attacking behaviors of Harris hawks on the prey in nature, such as preaching, predation, and surprise pounce strategies. Like other meta-heuristic algorithms, HHO includes two main phases: exploration and exploitation, However, HHO has two stages for exploration and four for exploitation, which described in detail as follows.

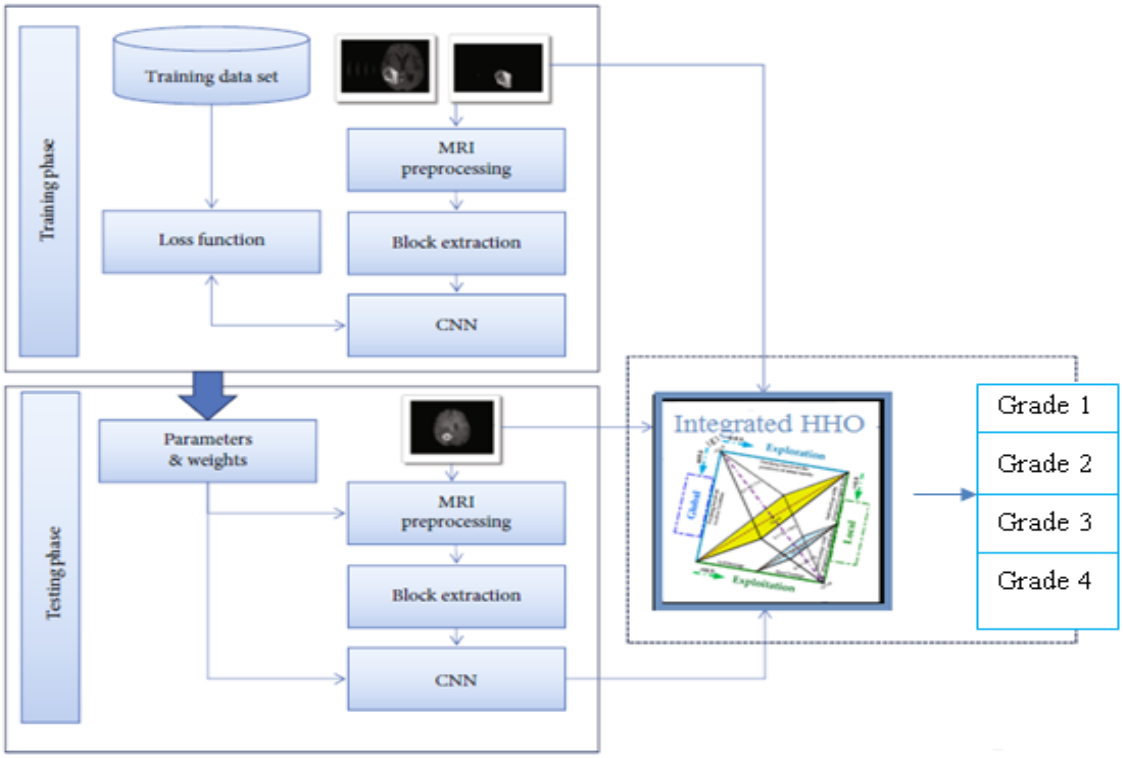

Figure 3: proposed HHO based CNN

Initialization Phase: In this phase, the objective function and its solution space are defined. In addition, the values for the parameters are assigned, and the initial population is created. Exploration Phase: It is the phase where Harris Hawks search for the prey (the rabbit). The hawks have compelling eyes that can help them to detect and track the prey, but it is sometimes difficult to see the prey. In this case, the hawks wait and monitor the site hoping to observe the prey. Practically, in each iteration all Harris hawks are the candidate solutions, and the fitness value is calculated for each of them based on the intended prey. After that, the Harris hawks may wait in some positions to detect the prey based on the following equation

$$X(t+1) = \begin{cases} X_{rand}(t) - r_1|X_{rand}(t) - 2r_2X(t)| & q \geq 0.5 \\ (X_{rabbit}(t) - X_m(t)) - r_3\big(LB + r_4(UB - LB)\big) & q \leq 0.5 \end{cases} \quad (7)$$

Where $X(t+1)$ is the position of hawks in the next iteration t, $X_{rabbit}(t)$ is the rabbit position, $X(t)$is the current position vector of the hawks, $X_m(t)$ refers to the average position of the current population of hawks. The variables r_1, r_2, r_3, r_4, and q (wait) are random numbers over the interval [0, 1], and LB and UB represent the upper and lower bounds of the problem variables. HHO uses a straightforward way to calculate the average position of hawks $X_m(t)$using the following equation

$$X_m(t) = \frac{1}{N}\sum_{i=1}^{N} X_i(t) \qquad (8)$$

where $X_i(t)$ refers to the position of the hawks in iteration t; and N represents the total number of hawks.

Transition From Exploration to Exploitation: It is critical to the performance of meta-heuristic algorithms to maintain the right balance between exploration and exploitation. In HHO, shifting between the exploration phase and exploitation phase, and between different exploitations depend on the prey escaping energy (E). HHO assumes that the energy of the rabbit is reducing during escaping from the hawks, which can be calculated as follows

$$E = E_0\left(1 - \frac{t}{T}\right) \qquad (9)$$

Where E is escaping energy, E_0 is the initial state of energy which its value randomly changes over the interval (-1, 1), and T is the maximum number of iterations. When the escaping energy of the rabbit $|E| \geq 1$, HHO redirects the hawks to explore different regions searching for the rabbit (exploration phase). However, when its energy is reduced$|E| < 1$, the hawks search the neighborhood for the solution during the exploitation phase.

Exploitation Phase: In this phase, Harris hawks attack the prey based on the position detected in the previous phase. However, the rabbit always attempts to escape, and the hawks follow the chasing strategy. Hence, HHO is designed based on four possible strategies of attacking techniques. Two variables indicate which strategy will be performed, r and$|E|$. While $|E|$ is the escaping energy of the rabbit, r refers to the probability of escaping, where r < 0:5 indicate a higher chance for the rabbit to escape successfully and $r \geq 0{:}5$ for failure to escape.

The EOBL technique is used to improve the global search ability of HHO. The opposition point is defined as follows: for the individual $X_i = (x_{i;1};\ x_{i;2};\ \ldots\ ;\ x_{i;D})$ in the current population $X_e = (x_{e;1};\ x_{e;2};\ \ldots\ ;\ x_{e;D})$, then the elite opposite point $\check{X}_i = (\check{x}_{i;1};\ \check{x}_{i;2};\ \ldots\ ;\ \check{x}_{i;D})$ can be mathematically modeled as

$$\check{x}_{i;j} = s \times \left(da_j + db_j\right) - x_{i,j} \qquad (10)$$

where $s \in [a_i, b_i], S \in U[0,1]$ S is a generalized factor. da_j and db_j are dynamic boundaries, which can be defined as

$$da_j = \min\left(x_{i;j}\right), \qquad db_j = \max(x_{i;j}) \qquad (11)$$

However, the corresponding opposite can exceed the search boundary $[a_i, b_i]$. To solve this matter, the transformed individual is assigned a random value within $[a_i, b_i]$as follows

$$.\ \check{x}_{i;j} = rand\left(a_j, b_j\right), \qquad if \check{x}_{i;j} < a_j || \check{x}_{i;j} > b_j \qquad (12)$$

HHO relies on the rabbit energy $|E|$ to shift from exploration to exploitation and to choose the current type of exploitation. It also uses the rabbit energy to prevent the hawks from falling in local optima. However, the rabbit escaping energy may rapidly change its

convergence towards the optimal solution, which may cause the hawks to trapped in local optima [21]. In this subsection, we explain the proposed three search strategies (TSS) (Mutation, Mutation Neighborhood Search (MNS) And Rollback Strategy) to enhance both of the global and local search mechanisms of the HHO algorithm. The advantage of the HHHO-CNN is feature concatenation that helps us to learn the features in any stage without the need to compress them and the ability to control and manipulate that features. This technique helps us to avoid the parameter number explosion so we reduce the training process complexity and eliminate the over fitting problem.

4. EXPERIMENTAL RESULTS AND ANALYSIS

- **Experimental Setup**

The proposed method has been implemented using the Matlab environment on Core 2 Duo, processor speed 1.6 GHz .The proposed system has been tested on the data set available at web [17]. The proposed system has been tested on the BRATS 2017 dataset with the size of "512 × 512" here 400 images are collected (4 sorts of evaluations) and each evaluation contains 100 images. It has also been tested on dataset of real brain MR images consisting of different grades of brain images.

- ***Confusion Matrix and Validation Metrics***

Confusion chart creates a confusion matrix chart from true labels true Labels and predicted labels predicted Labels and returns a Confusion Matrix Chart object. The rows of the confusion matrix correspond to the true class and the columns correspond to the predicted class. Diagonal and off-diagonal cells correspond to correctly and incorrectly classified observations, respectively. The performance of the classification model is often described by 'confusion matrix'. The elements of confusion matrix are as follows

- True Positives (TP): No. of Benign/ Malignant MR images those are classified as they are Benign/ Malignant.
- True Negatives (TN): No. of Non-Benign/ Non-Malignant MR images those are classified as they are Non-Benign/ Non-Malignant.
- False Positives (FP): No. of Non-Benign/ Non-Malignant images those are classified as they are Benign/ Malignant.
- False Negatives (TN): No. of Benign/ Malignant MR images those are classified as they are Non-Benign/ Non-Malignant

Here the validation metrics such as sensitivity, specificity, accuracy, precision and F-measure are evaluated. The mathematical representation of evaluation metrics are shown in (13-17).

$$\text{Sensitivity} = \frac{TP}{TP+FN} \times 100\% \quad (13)$$

$$\text{Specificity} = \frac{TN}{TN+FP} \times 100\% \quad (14)$$

$$\text{Accuracy} = \frac{TP+TN}{TP+FP+FN+TN} \times 100\% \quad (15)$$

$$\text{Precision} = \frac{TP}{TP+FP} \times 100\% \quad (16)$$

$$F - \text{measure} = \frac{2 * \text{Precision} * \text{Recall}}{\text{Pr ecision} + \text{Recall}} \quad (17)$$

- **Performance of classification phase**

Here two different classifiers are used such as SVM and BOVW classifier. Support vector machine (SVM) is one of the techniques used for the classification purpose. BOVW classifier's main purpose is to reduce the time consumption; this classifier will automatically select the features that accompany this classification. Here this both classifier, apply Harish Hawks Optimizer (HHO) methods by adjusting parameters such as weights and learning rates to reduce the loss. Table 1 shows the results of all experimentations.

Confusion matrix without optimization **Confusion matrix with optimization**

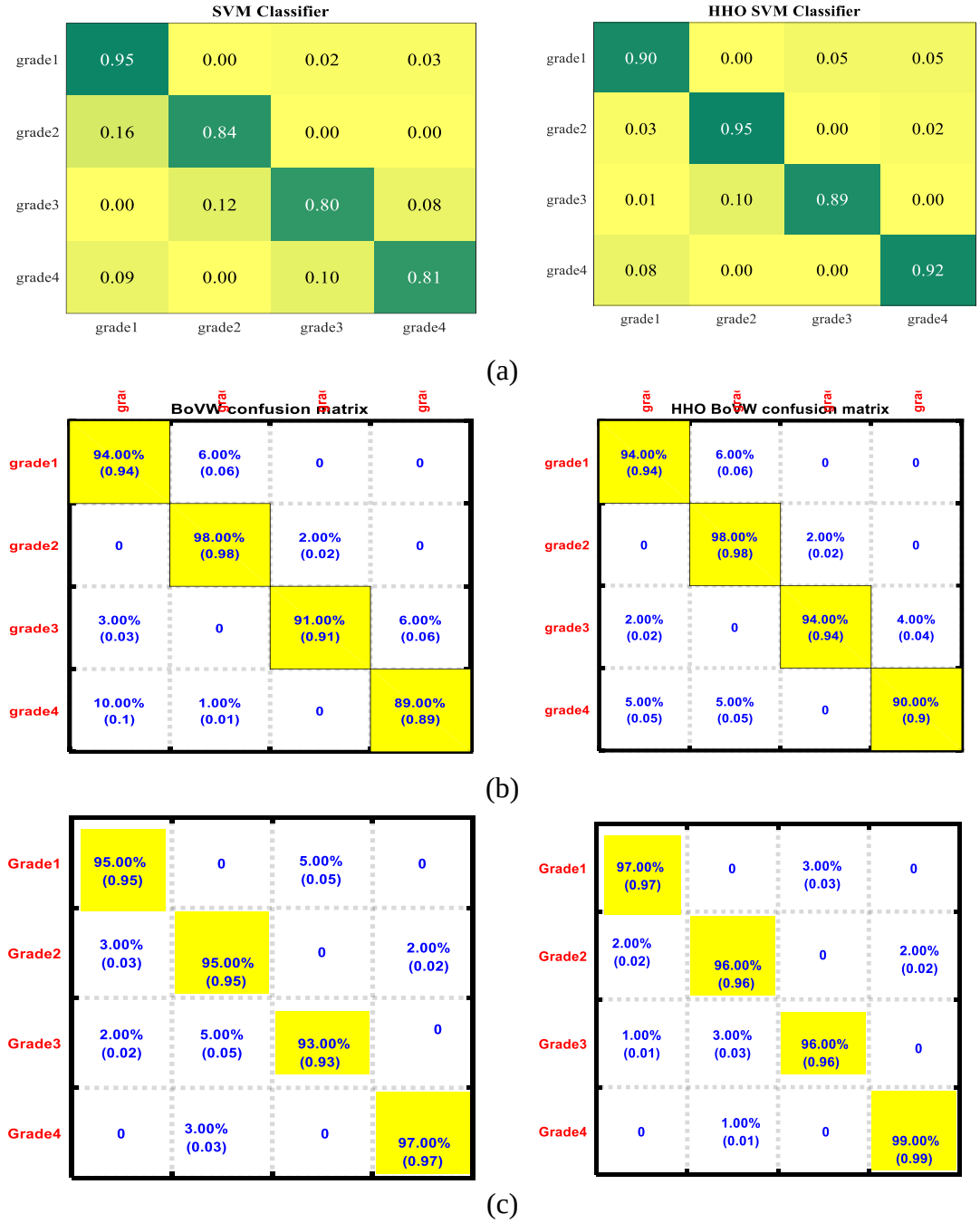

Figure 4: (a-c) confusion matrix of proposed Classifiers

Figure 4 shows the confusion matrix of SVM, BOVW and CNN classifiers with and without optimization in which classifiers classify the brain images based on the tetrolet and GLCM

features. The confusion matrix displays the total number of observations in each cell. The rows of the confusion matrix correspond to the true class, and the columns correspond to the predicted class. Diagonal and off-diagonal cells correspond to correctly and incorrectly classified observations, respectively. The diagonal area of the confusion matrix shows the perfect identification of benign and malignant images.

Table 1: performance value of classifiers

Metrics	*SVM*	*HHO-SVM*	*BOVW*	*HHO-BOVW*	*CNN*	*HHO-CNN*
Accuracy	0.8500	0.9150	0.93000	0.9400	0.95	0.97
Error	0.1500	0.0850	0.0700	0.0600	0.05	0.03
Sensitivity	0.8500	0.9150	0.9300	0.9400	0.95	0.97
Specificity	0.9500	0.9717	0.9767	0.9800	0.9833	0.99
Precision	0.8542	0.9158	0.9318	0.9416	0.95027	0.9699
F1-Score	0.8495	0.9150	0.9300	0.9400	0.95005	0.96997

Figure 5 shows the Accuracy, Error, Sensitivity, Specificity and Precision plot of proposed classifiers. From the bar chart the HHO based CNN classifiers obtains higher accuracy, sensitivity, precision and specifivcity; the error value is lower than the proposed classifiers, the outcomes prove that the performance the proposed algorithm is excellent. The application of the proposed method for early detection of tumor is demonstrated to improve efficiency and accuracy of clinical practice. The application of the proposed method for tracking tumor is demonstrated to help pathologists distinguish exactly tumor region and its type of tumor.

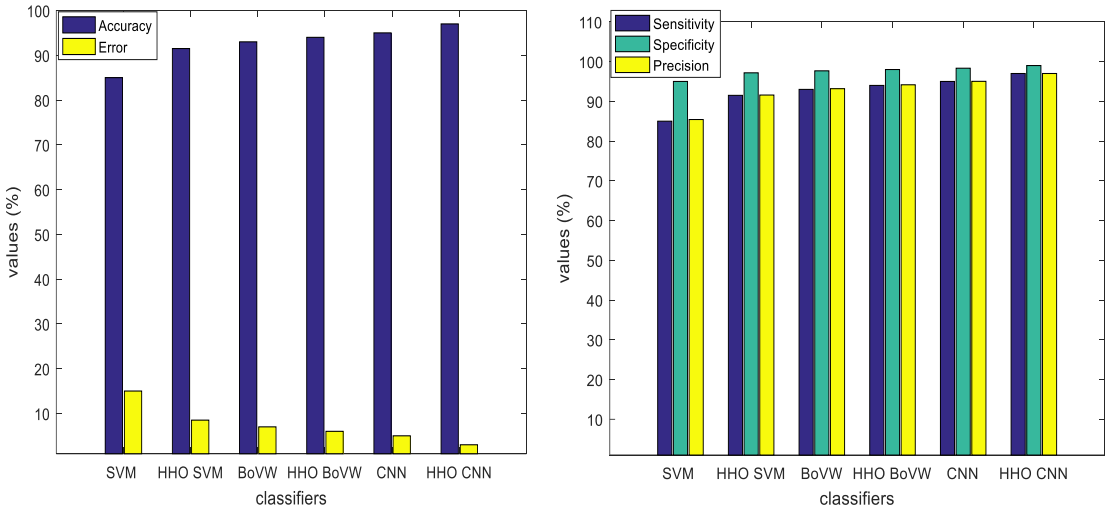

(a) (b)

Figure 5: (a & b) comparison plot of various classifiers

- **Comparative analysis with state of art-methods**

To prove the effectiveness of the proposed methodology, we compare our work with various published works listed in table 2. In this table [28], tumor image classification and segmentation was proposed. For classification, they used support vector machine. In [29], Combining PSO based SVM for tumor Detection and Segmentation over MRI were proposed.. Similarly, in [30], PNN algorithm based tumor detection is proposed.

Table 2: performance with state of art models

Methods	**Accuracy (%)**
Le et al.[28]	88
Sivapriya et al.[29]	92
Saritha et al[30]	93
Proposed techniques	
CNN	95
HHO-CNN	97

The comparison based result is given in Table 2. Table shows the comparative results of proposed against existing. When analyzing figure 4, our proposed methodology attain the maximum accuracy of 97% which is 88% for [29], 92% for [28] and 93% for [27]. From the graph we clearly understand, our proposed method attain the better result compared to other methods. Our model needs less computational specifications as it takes less execution time. Moreover, our model accuracy is much better than other models. Our proposed system can play a prognostic significance in the detection of tumors in brain tumor patients. Also, our proposed system can play an effective role in the early diagnosis of dangerous disease in other clinical domains related to medical imaging, particularly lung cancer and breast cancer whose mortality rate is very high globally. We can prolong this approach in other scientific areas as well where there is a problem in the availability of large data or we can use the different transfer learning methods with the same proposed technique.

5. CONCLUSION AND FUTURE WORK

In the context of classification, deep convolutional neural networks (CNNs) have been widely proven in the scientific and industrial community. Here, investigated the performance of a deep neural network model on a classification task related to brain cancer detection. The modification applied to the ResNet-50 model proves that deep learning model used in natural images processing can achieves high performance in medical images processing. In our case we achieve about 97% of accuracy in the optimized brain tumor classification task and that outperform human expert in the diagnostic domain. The performance achieved can be improved if we provide more data using larger datasets. In this work an efficient methodology which combines the HHO with the Convolutional Neural Network (CNN) to classify the brain MRIs into different grades of Astrocytoma. In addition using this classifier shows high accuracy compared to traditional classifiers. To further boost the model efficiency, different architecture and comprehensive hyper-parameter tuning technique can be conceived.

REFERENCES

1. Hollon, Todd C., Balaji Pandian, Arjun R. Adapa, Esteban Urias, Akshay V. Save, Siri Sahib S. Khalsa, Daniel G. Eichberg et al. "Near real-time intraoperative brain tumor diagnosis using stimulated Raman histology and deep neural networks." *Nature medicine* 26, no. 1 (2020): 52-58.
2. Hamerla, Gordian, Hans-Jonas Meyer, Stefan Schob, Daniel T. Ginat, Ashley Altman, Tchoyoson Lim, Georg Alexander Gihr, Diana Horvath-Rizea, Karl-Titus Hoffmann, and Alexey Surov. "Comparison of machine learning classifiers for differentiation of grade 1 from higher gradings in meningioma: A multicenter radiomics study." *Magnetic resonance imaging* 63 (2019): 244-249.
3. Arunkumar, N., Mazin Abed Mohammed, Salama A. Mostafa, Dheyaa Ahmed Ibrahim, Joel JPC Rodrigues, and Victor Hugo C. de Albuquerque. "Fully automatic model-based segmentation and classification approach for MRI brain tumor using artificial neural networks." *Concurrency and Computation: Practice and Experience* 32, no. 1 (2020): e4962.
4. Pugalenthi, R., M. P. Rajakumar, J. Ramya, and V. Rajinikanth. "Evaluation and classification of the brain tumor MRI using machine learning technique." *Journal of Control Engineering and Applied Informatics* 21, no. 4 (2019): 12-21.
5. Qian, Zenghui, Yiming Li, Yongzhi Wang, Lianwang Li, Runting Li, Kai Wang, Shaowu Li et al. "Differentiation of glioblastoma from solitary brain metastases using radiomic machine-learning classifiers." *Cancer Letters* 451 (2019): 128-135.
6. Iqbal, Sajid, Muhammad U. Ghani Khan, Tanzila Saba, Zahid Mehmood, Nadeem Javaid, Amjad Rehman, and Rashid Abbasi. "Deep learning model integrating features and novel classifiers fusion for brain tumor segmentation." *Microscopy research and technique* 82, no. 8 (2019): 1302-1315.
7. Chaplot, S.; Patnaik, L.M.; Jagannathan, N.R. (2006). Classification of magnetic resonance brain images using wavelets as input to support vector machine and neural network, Biomed. Signal Process Control, 1, 86–92. 3. Maitra, M.: Chatterjee, A. (2011).
8. A Slantlet transform based intelligent system for magnetic resonance brain image classification. Biomed. Signal Process Control, 1, 299–306.
9. Zhang, Y.; Wu, L.; Wang, S. (2011). Magnetic resonance brain image classification by an improve artificial bee colony algorithm. Progress Electromagnetic Resolution, 116, 65–79.
10. Naik, J.; Prof. Patel, Sagar (2013). Tumor Detection and Classification using Decision Tree in Brain MRI. IJEDR , ISSN:2321-9939.
11. Zhang, Y. and Wu, L. (2012). An MR Brain Images Classifier via Principal Component Analysis and Kernel Support Vector Machine. Progress in Electromagnetic Research, Vol.130, 369-388
12. A.R. Mathew, P.B. Anto, N.K. Thara Brain tumor segmentation and classification using DWT, Gabour wavelet and GLCM Intelligent Computing, Instrumentation and Control Technologies (ICICICT), 2017 International Conference on IEEE (2017), pp. 1744-1750
13. S. Iqbal, M.U. Ghani, T. Saba, A. Rehman Brain tumor segmentation in multi-spectral MRI using convolutional neural networks (CNN) Microsc Res Tech, 81 (4) (2018), pp. 419-427

14. . Sharif M.I., Li J.P., Khan M.A., Saleem M.A. Active deep neural network features selection for segmentation and recognition of brain tumors using MRI images. Pattern Recognit. Lett. 2020;129:181–189. doi: 10.1016/j.patrec.2019.11.019.
15. Arunkumar N., Mohammed M.A., Mostafa S.A., Ibrahim D.A., Rodrigues J.J., de Albuquerque V.H.C. Fully automatic model-based segmentation and classification approach for MRI brain tumor using artificial neural networks. Concurr. Comput. Pract. Exp. 2020;32:e4962. doi: 10.1002/cpe.4962.
16. Sharif M., Amin J., Raza M., Anjum M.A., Afzal H., Shad S.A. Brain tumor detection based on extreme learning. Neural Comput. Appl. 2020:1–13. doi: 10.1007/s00521-019-04679-8.
17. Ismael S.A.A., Mohammed A., Hefny H. An enhanced deep learning approach for brain cancer MRI images classification using residual networks. Artif. Intel. Med. 2020;102:101779. doi: 10.1016/j.artmed.2019.101779.
18. Sharif M., Tanvir U., Munir E.U., Khan M.A., Yasmin M. Brain tumor segmentation and classification by improved binomial thresholding and multi-features selection. J. Amb. Intel. Hum. Comp. 2018:1–20. doi: 10.1007/s12652-018-1075-x.
19. Khan M.A., Lali I.U., Rehman A., Ishaq M., Sharif M., Saba T., Zahoor S., Akram T. Brain tumor detection and classification: A framework of marker-based watershed algorithm and multilevel priority features selection. Microsc. Res. Tech. 2019;82:909–922. doi: 10.1002/jemt.23238.
20. Ke Q., Zhang J., Wei W., Damaševičius R., Woźniak M. Adaptive independent subspace analysis of brain magnetic resonance imaging data. IEEE Access. 2019;7:12252–12261. doi: 10.1109/ACCESS.2019.2893496.
21. Rehman A., Naz S., Razzak M.I., Akram F., Imran M. A deep learning-based framework for automatic brain tumors classification using transfer learning. Circ. Syst. Signal. Pr. 2020;39:757–775. doi: 10.1007/s00034-019-01246-3.
22. Ghosal P., Nandanwar L., Kanchan S., Bhadra A., Chakraborty J., Nandi D. Brain Tumor Classification Using ResNet-101 Based Squeeze and Excitation Deep Neural Network; Proceedings of the Second International Conference on Advanced Computational and Communication Paradigms (ICACCP); Gangtok, India. 25–28 February 2019; pp. 1–6.
23. Chuang, Tzu-Yi, Jen-Yu Han, Deng-Jie Jhan, and Ming-Der Yang. "Geometric Recognition of Moving Objects in Monocular Rotating Imagery Using Faster R-CNN." *Remote Sensing* 12, no. 12 (2020): 1908.
24. Ćiprijanović, Aleksandra, G. F. Snyder, Brian Nord, and Joshua EG Peek. "DeepMerge: Classifying high-redshift merging galaxies with deep neural networks." *Astronomy and Computing* 32 (2020): 100390.
25. Sarhan, Ahmad M. "Detection and Classification of Brain Tumor in MRI Images Using Wavelet Transform and Convolutional Neural Network." *Journal of Advances in Medicine and Medical Research* (2020): 15-26.
26. Chaubey, Nirbhay Kumar, and Prisilla Jayanthi. "Disease Diagnosis and Treatment Using Deep Learning Algorithms for the Healthcare System." In *Applications of Deep Learning and Big IoT on Personalized Healthcare Services*, pp. 99-114. IGI Global, 2020.
27. Sihwail, Rami, Khairuddin Omar, Khairul Akram Zainol Ariffin, and Mohammad Tubishat. "Improved Harris Hawks Optimization Using Elite Opposition-Based Learning and Novel Search Mechanism for Feature Selection." *IEEE Access* 8 (2020): 121127-121145.

28. Le Trung., Dat Tran, Wanli Ma, and Dharmendra Sharma, A new support vector machine method for medical image classification. In Visual Information Processing (EUVIP), 2010 2nd European Workshop on. IEEE, 2010, 165–170.
29. Sivapriya TR., AR Nadira Banu Kamal, and V Thavavel, Automated classification of MRI based on hybrid Least Square Support Vector Machine and Chaotic PSO. In Computing Communication & Networking Technologies (ICCCNT), 2012 Third International Conference on. IEEE, 2012, 1–7.
30. Saritha M., K Paul Joseph, and Abraham T Mathew (2013). Classification of MRI brain images using combined wavelet entropy based spider web plots and probabilistic neural network. Pattern Recognition Letters, 34(16), 2151–2156.